Supplementary Information

Spatial compartmentation and food web stability

A. Mougi

Supplementary Figures

To examine the robustness of the results in Fig. 2a and 2b, I used different stability index, network topology, connectance, or species richness. First, the stability is evaluated by resilience (engineering resilience), namely, the rate of recovery to original equilibrium after a small perturbation, which is calculated by the mean magnitude of the real part of the dominant eigenvalue of J across 1000 samples of locally stable communities (Fig. S1). Second, cascade model is used as other network type (Fig. S2). In the cascade model, for each pair of species, $i, j = 1,\ldots, n$ with $i < j$, species i never consumes species j, whereas species j may consume species i. Third, different values of C (Fig. S3) and N (Fig. S4) are considered. Even if I change these factors, we can see that the results in Fig. 2a, b are qualitatively unchanged. However, in larger N, larger M tends to decrease the stability than in smaller N.

In addition to these changes, I relax strong assumptions of symmetry of parameters. First is the proportions of migratory species in sub-food webs ($p_1 = p_3 = p$ in the main text). As shown in Fig. S5, even if the change of p_1 (p_3 is fixed) almost do not affect the result. Second is the community sizes of each original habitat, which are controlled by the proportion of species in sub-food web 1, q_1 ($q_3 = 1 - q_1$). In the main text, $q_1 = q_3 = q$. As shown in Fig. S6, even if the change of q_1 (q_3 is fixed) almost do not affect the result.

Fig. S1. Relationships between spatial coupling strength and resilience with varying proportions of migratory species. (a) Boundary-separated subsystems. (b) Globally-connected subsystems. Other information is the same as in Fig. 2a, b.

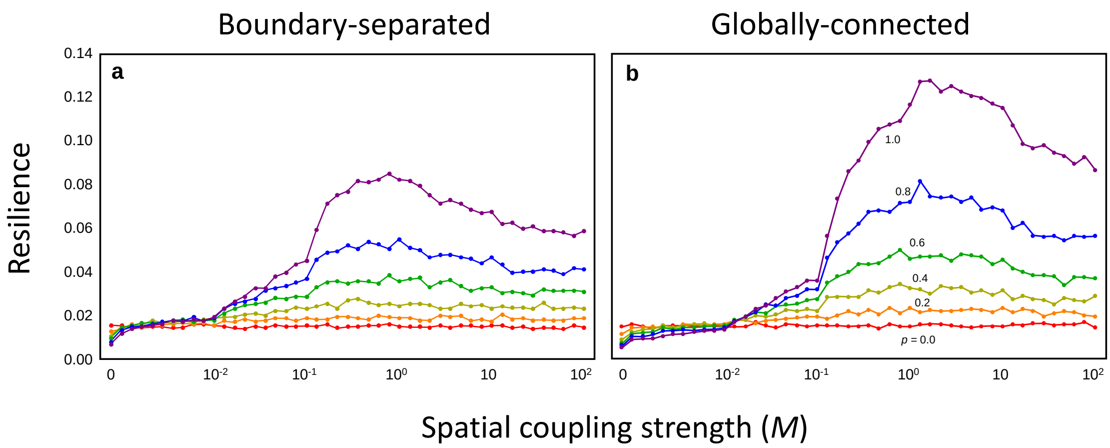

Fig. S2. Relationships between spatial coupling strength and stability with varying proportions of migratory species in a cascade model. (a) Boundary-separated subsystems. (b) Globally-connected subsystems. Other information is the same as in Fig. 2a, b.

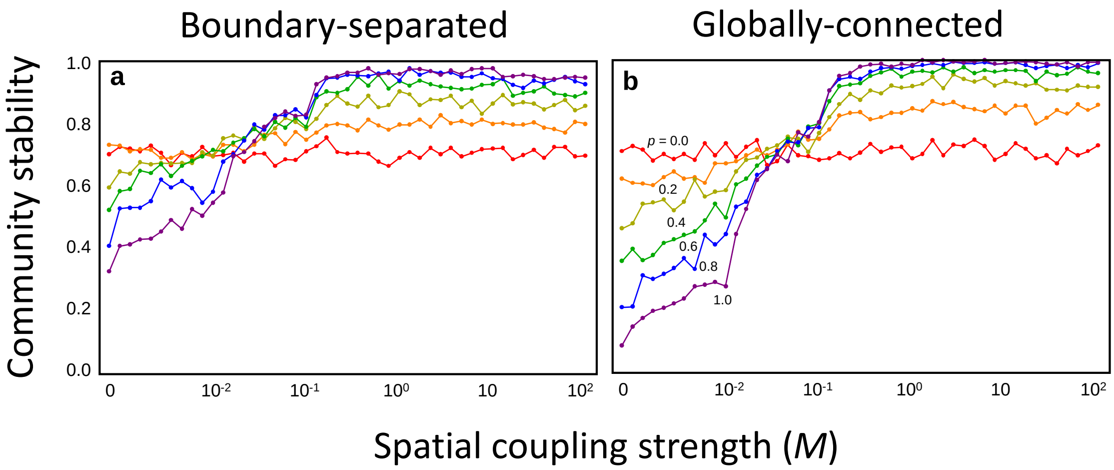

Fig. S3. Relationships between spatial coupling strength and stability with varying proportions of migratory species. (a, b) Boundary-separated subsystems. (c, d) Globally-connected subsystems. In (a) and (c), C = 0.75. In (b) and (d), C = 0.25. Other information is the same as in Fig. 2a, b.

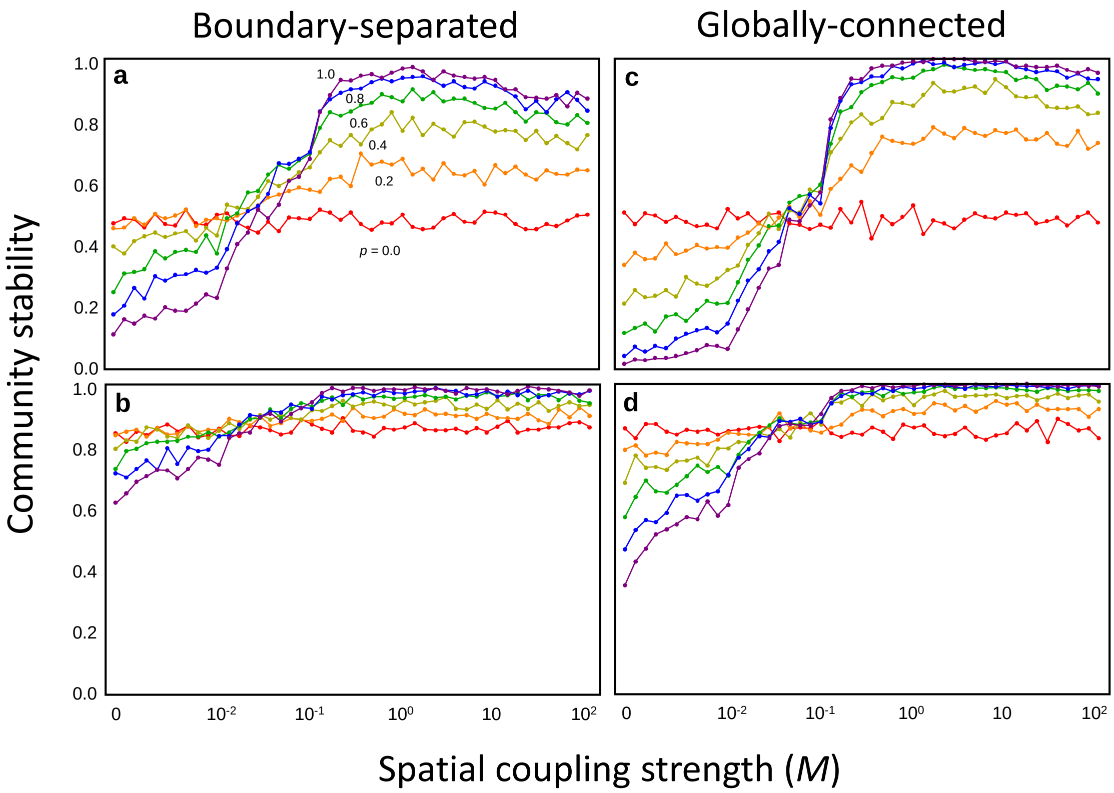

Fig. S4. Relationships between spatial coupling strength and stability with varying proportions of migratory species. (a, b) Boundary-separated subsystems. (c, d) Globally-connected subsystems. In (a) and (c), N = 100. In (b) and (d), N = 20. Other information is the same as in Fig. 2a, b. Note that the stability almost does not change even in $M = 10^{10}$.

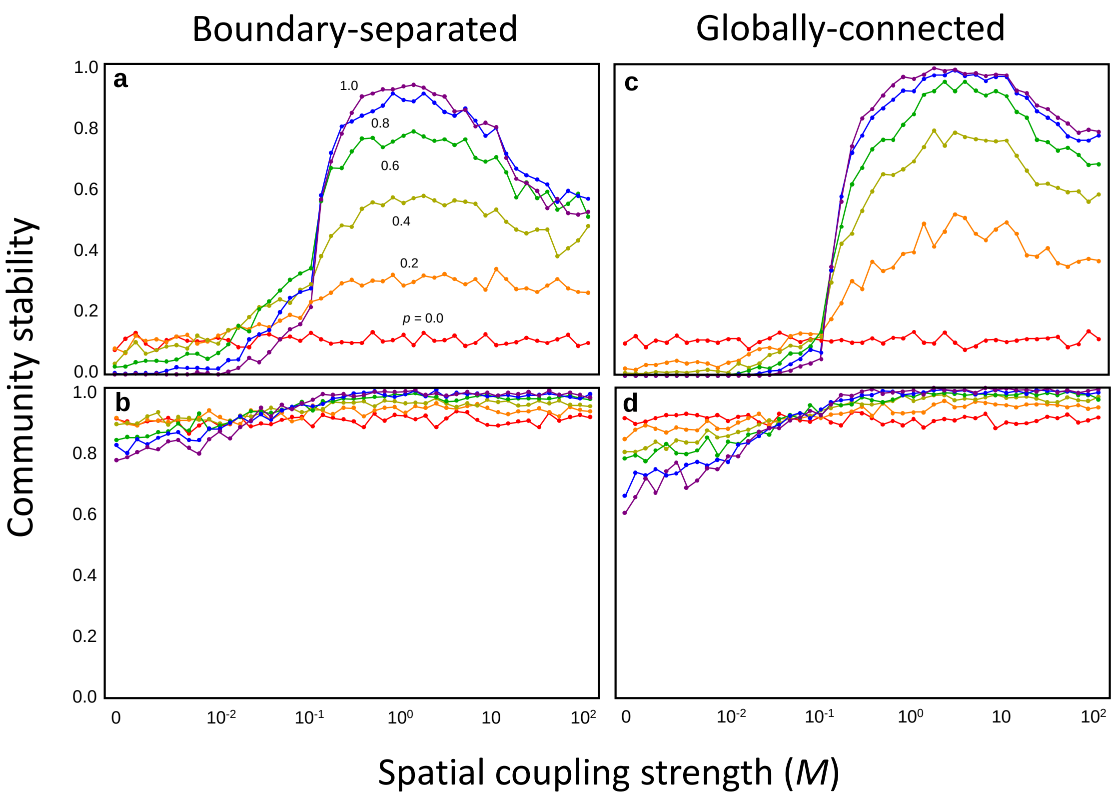

Fig. S5. Relationships between spatial coupling strength and stability with varying proportions of migratory species in a patch 1 (p_1). (a) Boundary-separated subsystems. (b) Globally-connected subsystems. p_2 = 0.5. Other information is the same as in Fig. 2a, b.

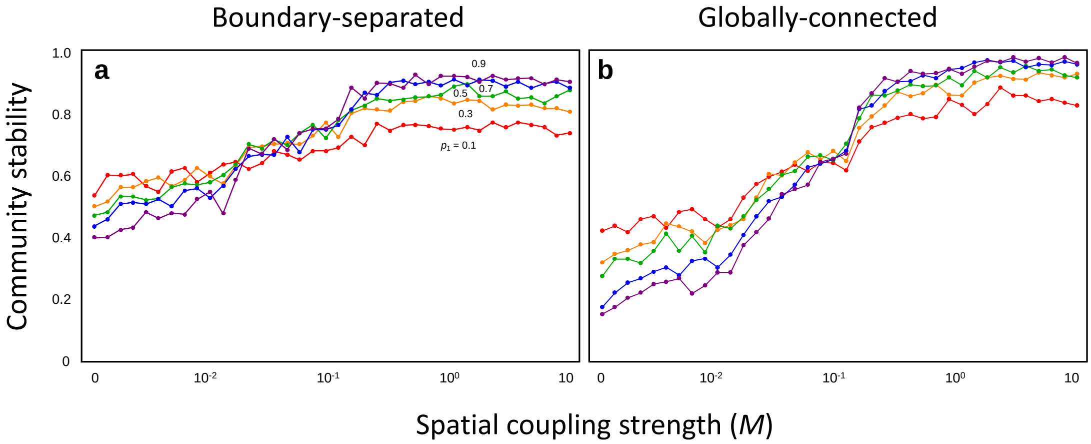

Fig. S6. Relationships between spatial coupling strength and stability with varying q_1. (a) Boundary-separated subsystems. (b) Globally-connected subsystems. Other information is the same as in Fig. 2a, b.